2015-03-31

Shielding technique for deposition of Au electrical contacts on graphene by sputtering

Li, B

10.1116/1.4916589
JOURNAL OF VACUUM SCIENCE & TECHNOLOGY A
American Vacuum Society

Shielding technique for deposition of Au electrical contacts on graphene by sputtering

Bing Li[a] and Genhua Pan
Wolfson Nanomaterials and Devices Laboratory, Faculty of Science and Technology, University of Plymouth, Devon PL4 8AA, United Kingdom and Centre for Research in Translational Biomedicine, Faculty of Science and Technology, University of Plymouth, Devon PL4 8AA, United Kingdom

Nawfal Y. Jamil, Laith Al Taan, and Shakil Awan
Wolfson Nanomaterials and Devices Laboratory, Faculty of Science and Technology, University of Plymouth, Devon PL4 8AA, United Kingdom

Neil Avent
Centre for Research in Translational Biomedicine, Faculty of Science and Technology, University of Plymouth, Devon PL4 8AA, United Kingdom

(Received 20 January 2015; accepted 19 March 2015; published 31 March 2015)

Here, the authors report on a novel shielding technique for the fabrication of electrical contacts on exfoliated graphene by sputtering and lift-off process. The technique solves this problem by removing unwanted gold film in patterning contacts and reduces the high contact resistivity typically found in sputtered devices ranging from 260 to 940 kΩ μm induced by sputtered Au on graphene. By using a shielding tube integrated into our sputtering machine and optimizing the sputtering parameters, contact resistivity as low as 1.04 kΩ μm has been achieved. Consequently, the total device resistivity is significantly reduced, and the yield rate of the devices fabrication has also increased from 17% to 90%. © *2015 American Vacuum Society*. [http://dx.doi.org/10.1116/1.4916589]

I. INTRODUCTION

Graphene, a two-dimensional honeycomb sp^2-hybridized carbon, has attracted a huge amount of interest since its experimental discovery in 2004.[1] To explore its unique properties in biological, electrical and thermal applications[2–5] and ultimately to apply them to the industrial scale applications, a nondestructive large-scale method for forming contacts on graphene films is urgently required. Although many approaches have been proposed and demonstrated in laboratories, such as e-beam evaporation,[6] chemical vapor deposition,[7] and thermal evaporation,[8] only the latter has been considered as the nondestructive deposition tool for the fabrication of graphene devices. As the main preferred deposition technique in the semiconductor industry, sputtering has numerous advantages such as high throughput, diverse material choices, etc. However, the energetic sputtering flux deposited onto a graphene film always induces defects and disorders, resulting in the high contact resistance in graphene field effect transistors (FETs).[9–12] Moreover, without the assistance of ultrasonic bath, it is impossible to fabricate contacts on graphene by lift-off process if the Au films were deposited by sputtering due to the difficulties in removing the unwanted Au films in the subsequent lift-off process. However, sonication should be avoided in the process for the fabrication of graphene devices due the potential damage, which it can cause to graphene.[13]

Prior to our work, the deposition of sputtered Au films leading to low-defect graphene has been attempted by two groups using improved sputtering configurations.[14,15] According to their reports, both the sample flipping and the low incidence were effective in reducing damage to graphene caused by sputtering deposition. However, the flipping configuration or the low sputtering angle makes the practical lift-off process more difficult to achieve; hence, no electrical measurements of devices have been reported in these studies.[3]

In this paper, we have developed a novel shielding technique for forming Au contacts on graphene. To our knowledge, this is the first method reported so far for the deposition of Au contacts on graphene without causing any problems in the lift-off process. Different sputtering conditions, such as Ar pressure and discharge power, have been systematically investigated and optimized to decrease the damage from sputtered Au. Compared with those devices prepared with normal sputtering deposition, the devices prepared with using our supplementary shielding tube and optimized deposition conditions show an improved yield success from 17% to 90% during fabrication process; the corresponding two-probe contact resistivity ($R_{contact}$) and total device resistivity (R_{total}) reduced to 1.04 and 2.4 kΩ μm, respectively.

II. EXPERIMENT

Graphene samples were prepared with mechanical exfoliation from highly oriented pyrolytic graphite and transferred

[a]Electronic mail: bing.li@plymouth.ac.uk

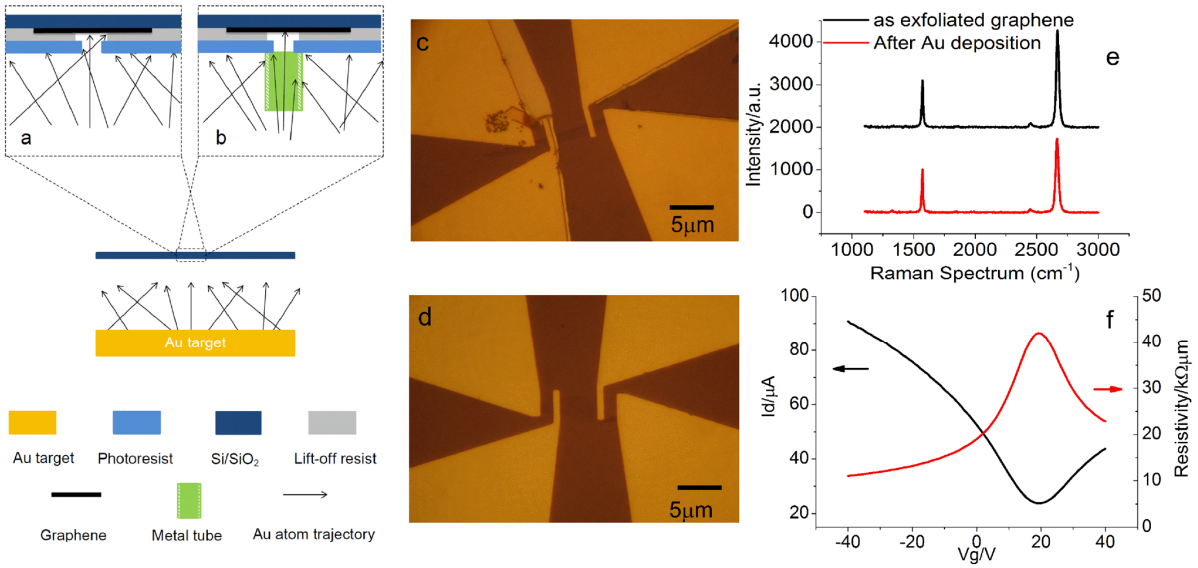

FIG. 1. (Color online) Schematic illustration of different sputtering configurations, optical microscope images and characteristics of the corresponding devices. (a) Configuration of normal sputtering. (b) Configuration of using a home-made shielding tube with sputtering. (c) and (d) Optical images of the devices prepared with normal and tube installed configurations, respectively (both c and d taken at 50× magnification, scale bar is 5 μm). (e) Raman spectra obtained from as-exfoliated graphene (top) and graphene underneath the sputtered Au contacts (bottom), respectively. 1f. I_d-V_g (left) and R-V_g (right) characteristics of a graphene FET, source–drain voltage is 500 mV. The Au contacts in (e) and (f) are sputtered with using the shielding tube at a discharge power of 20 W and Ar pressure of 20 mT.

onto a highly B-doped Si substrate with a 300 nm thermally oxidized SiO_2 layer on top. The quality and the layer number of graphene was evaluated by a combination of optical microscopy[16,17] and Raman spectroscopy.[17,18]

Samples were then cleaned in the vacuum chamber of the sputtering machine for 1 h to remove any gaseous molecules and water molecules physically absorbed on the graphene surface. For lift-off process with dual-layer resist, samples were spin-coated with a 0.5 μm-thick lift-off resist (LoR) followed by a 0.5 μm-thick photoresist.[19] The undercut distance is 0.2 μm after development. This optimized LoR distance is not able to overcome difficulties in removing unwanted Au film, but can be used to help achieve better-defined contact edges. Au film was sputter-deposited after the photolithographic patterning.

The sputtering deposition of Au contacts was carried out with using a shielding tube as detailed in Sec. III. The inner diameter of the shielding tube is Φ14 with a height of 20 mm. The four contact patterns have an overall size of 5 mm × 5 mm and the channel length is constant and kept as 2 μm for all devices used in this paper. This optimized dimension could not only provide an adequate deposition rate of the Au film, but also prevent the deposition of Au film onto the side walls of the photoresist. Approximately 30–50 nm Au film was deposited onto graphene as the contact material in a three-target sputtering machine. Base vacuum was 2×10^{-7} Torr and Ar pressure for deposition was 4–20 mTorr depending on the specific samples. Back water cooling was applied to the substrate during the sputtering process.

Surface morphologies of the FET devices were characterized by the optical microscope and the atomic force microscope. Quality of graphene film underneath the Au contacts and in the channel area was evaluated by Raman Spectroscopy equipped with a 532 nm laser. Electronic characteristics of graphene FETs were measured with the Keithley 2602A multichannel source/measurement meter under ambient environmental conditions. The contact resistivity of all devices has been extracted at a high negative V_g (Ref. 20) and is found to have a discrepancy of 10%–15%, compared with that contact resistivity extracted through least-square curve fitting of the I_{sd} vs V_g (Ref. 21) or transfer length measurement.[22]

III. RESULTS AND DISCUSSION

A. Fabrication of Au contacts

Figures 1(a) and 1(b) show the normal and the tube shielding sputtering configuration for the deposition of Au contacts on graphene, respectively. When the Au film is deposited with the normal sputtering configuration [as shown in Fig. 1(a)], the film is also deposited onto the side walls of the photoresist right through to the surface of graphene even with the presence of undercuts created by LoR, where it links up all the contacts and causes difficulties in removing the unwanted Au film in the lift-off process. The optical microscope image in Fig. 1(c) shows a typical lift-off result for samples prepared with the normal configuration, where two electrical contacts are still connected with each other by the Au film bridge, leading to a short circuit in electrical measurements. The micron-sized Au ribbon suspended at the edge of the contacts results in a fluctuation in the $R_{contact}$.

This phenomenon became more serious when the pattern size is reduced to few micrometers.

To overcome this problem, we have proposed that a shielding tube be used together with normal sputtering, as shown in Fig. 1(b). An aluminum tube acting as a shield is mounted on top of the patterned substrate. The bore size of this tube is slightly bigger than the photoresist patterns to prevent Au atoms from depositing onto the photoresist side walls. In this case, only a small portion of sputtered Au atoms could reach the surface of graphene via the perpendicular trajectories, resulting in the sharp and clean patterns of electrical contacts after lift-off, as shown in Fig. 1(d). The fabrication yield for the lift-off step consequently increased from 17% to nearly 90% using this technique.

Figure 1(e) presents the typical Raman spectra obtained before (top) and after (bottom) the deposition of Au contacts on graphene with the optimized conditions, respectively. It can been seen that D/G intensity ratio, which indicates the level of defects, increased from 0.01 to 0.04 after the deposition of sputtered Au contacts, suggesting that some limited number of defects have been introduced (the detailed damage analysis with change in sputtering conditions is discussed in Fig. 2). A typical I_d-V_g characteristic from the device prepared using the shielding tube, measured under the ambient conditions, is given in Fig. 1(f) (black). A good modulation of the channel conductivity can be seen together with a R_{total} of 15.6 kΩ μm, when a 500 mV source–drain voltage is applied, confirming the reasonably good electrical characteristics of our exfoliated grapheme.[23,24] The positively shifted Dirac point (minimum conductivity point) is attributed to the polymer residues and gaseous adsorbents trapped on the surface on graphene and the SiO_2/graphene interface, which act as p-type doping source. The corresponding $R_{contact}$ of 5.4 kΩμm can be quantitatively extracted from its R-V_g characteristic [shown in Fig. 1(f) red]. The minimum $R_{contact}$ of 1.04 kΩ μm has been recorded in this work, which is much lower than those obtained from devices prepared with normal sputtering configuration and comparable with those prepared with electron beam melting (EBM),[25] confirming the advantage of this technique in improving the device performance.

B. Comparison of damage to graphene by Au deposited with various sputtering parameters

The damage to graphene introduced by the sputtering deposition with using shielding tube and its impact on electron transport properties of devices was further investigated in order to optimize the deposition process. Figure 2(a) shows the effects of the different sputtering Ar pressures (4, 8, and 20 mTorr, respectively) to Raman spectra of the graphene underneath the Au contacts deposited with a discharge power of 50 W. When Au film was deposited at an Ar pressure of 4 mTorr [the top spectrum in Fig. 2(a)], wide D and G bands (D/G intensity ratio is 1.08) can be seen together with a negligible 2D band. By doubling the Ar pressure to 8 mTorr [the middle spectrum in Fig. 2(a)], the three characteristic bands of graphene (D band around 1350 cm^{-1}, G band 1580 cm^{-1}, and 2D 2680 cm^{-1}) were observed, presenting a D/G intensity ratio of 2.1 and a G/2D intensity ratio of 1.2. When Ar pressure further increased to 20 mTorr [the bottom spectrum in Fig. 2(a)], the three characteristic bands of graphene were maintained, and there was a sharp decrease of the D/G intensity ratio from 2.1 to 0.62. These results indicate that a higher Ar pressure is preferred in minimizing the damage to graphene, which agrees with the results reported by Chen *et al.*[14] using a grazing-angle sputtering configuration. The damage to graphene introduced by the sputtered Au film at the lower Ar pressure is mainly caused

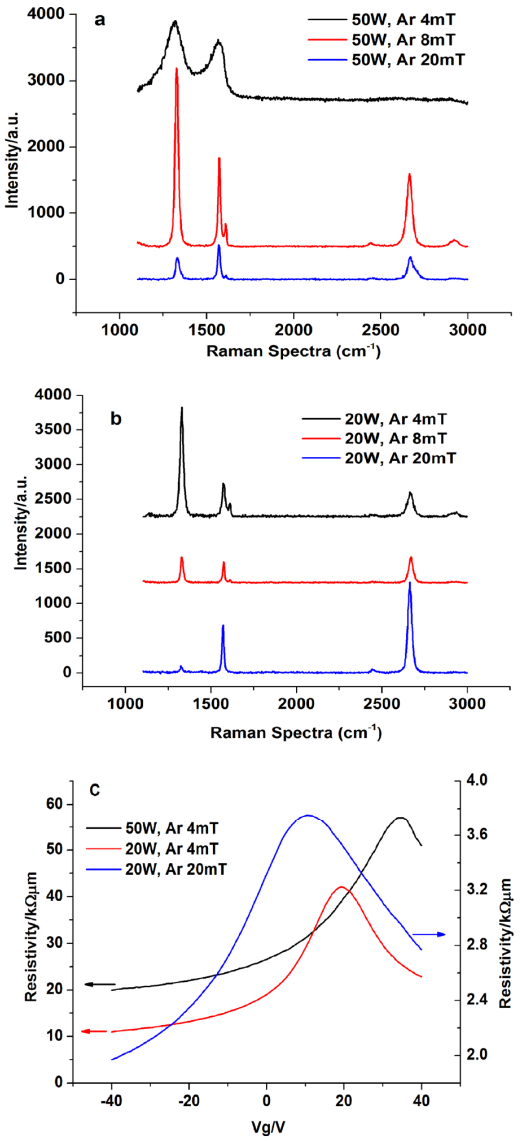

FIG. 2. (Color online) Raman spectra obtained from graphene underneath the Au contacts (5 nm gold) and the electronic measurements of the corresponding devices. Raman Spectra for contacts deposited at a discharge power of (a) 50 W and (b) 20 W, in both cases, three different Ar pressures (mTorr) were used. (c) Comparison of R-Vg characteristics of typical devices prepared with different sputtering conditions.

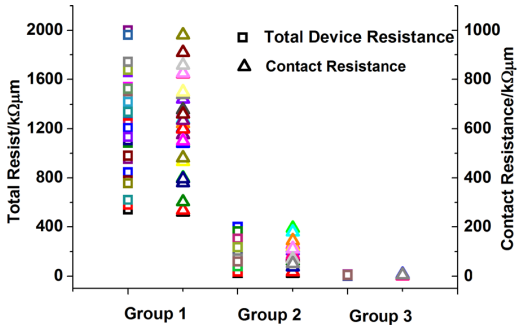

FIG. 3. (Color online) Statistics of success rate, total resistance (square), and contact resistance (triangle) of devices prepared with normal sputtering configuration (group 1), with using shielding tube (group 2), and the combination of shielding tube and optimized conditions (group 3), respectively.

by the bombardment of high speed energetic Au atoms, resulting in the amorphization of the sp^2-hybrided graphene crystals.[26] The higher Ar pressure increases the probability of interparticle collision, resulting in more disordered and random trajectories of sputtered species and in turn moderating the damage to graphene. And in this case, the crystals of graphene have been turned into nanocrystalline graphite (nc-G phase).[27] However, the deposition rate of sputtered Au decreases along with the increase of Ar pressure, from 11 nm/min at 4 mTorr to 0.6–0.7 nm/min at 20 mTorr with a discharge power of 50 W. Therefore, there is a limit on the maximum Ar pressure, above which the deposition rate is too low to be of any practical use.

Figure 2(b) shows a further set of Raman spectra obtained from the devices prepared at the same Ar pressures but with a reduced discharge power of 20 W. When the Ar pressure was increased from 4 to 8 and to 20 mTorr, D/G intensity ratio reduced from 3.36 in the top spectrum to 1.22 in the middle one and to 0.08 in the lower one. In comparison with the corresponding samples in Fig. 2(a) prepared at the same Ar pressures, the three characteristic bands of graphene and the lower D/G intensity ratios were preserved in all the three spectra. These results indicate that the decrease of sputtering power is also effective in reducing the damage to graphene caused by the deposition of sputtered Au film. The mechanism here is that the lower discharge power results in the less energetic Au atoms to arrive onto the surface of graphene; therefore, the damage caused by the bombardment of Au atoms is reduced. And under the optimized conditions of the Ar pressure and the discharge power, it can be seen that very little damage is introduced onto the graphene underneath the sputtered Au contacts [as shown in the lower spectrum in Fig. 2(b)].

Figure 2(c) provides a comparison of electron transport measurements obtained from the devices prepared with and without optimization of deposition conditions. When a discharge power of 50 W and an Ar pressure of 4 mTorr are used for the deposition of Au contacts [corresponding to the top spectrum in Fig. 2(a)], the electron transport characteristic shows a Dirac point around 35 V, a R_{total} of 26 kΩ μm and a calculated $R_{contact}$ of 10 kΩ μm [black curve in Fig. 2(c)]. In contrast, the electron transport characteristic of the device contacts prepared with a decreased discharge power of 20 W [corresponding to the top spectrum in Fig. 2(b)] shows a positively shifted Dirac point at 20 V, a decreased R_{total} of 16 kΩ μm and a decreased $R_{contact}$ of 5.6 kΩ μm [red curve in Fig. 2(c)]. By using a decreased discharge power of 20 W and an increased Ar pressure of 20 mTorr at same time [corresponding to the lower spectrum in Fig. 2(b)], a further positively shifted Dirac point at 10 V, a decreased R_{total} of 3.4 kΩ μm and a decreased $R_{contact}$ of 1.04 kΩ μm were obtained [blue curve in Fig. 2(c)]. These results suggest that the damage to graphene crystal/lattice structure, which is attributed to the deposition of Au contacts on top, leads to the disorder of graphene lattice under the Au contacts, which in turn leads to the higher $R_{contact}/R_{total}$ and the higher doping level of graphene FET. Lower discharge power and higher Ar pressure for the deposition of Au contacts are preferred to minimize the damage to graphene, therefore maintaining its unique electronic properties.

C. Device yield rate and total device resistance

Following characterizations of 75 graphene FETs, the statistical success or yield rate of device fabrication (the number of devices with clearly patterned/separated metal contacts to the total number of devices fabricated), R_{total} and $R_{contact}$ of the devices prepared under different configurations and sputtering conditions are presented in Fig. 3. It can be seen that a low fabrication yield rate of 17%, a R_{total} range of 540 kΩ μm–2 MΩ μm and a $R_{contact}$ range of 260–940 kΩ μm result due to the lift-off problem and the deposition of Au contacts under normal sputtering configuration. When the shielding tube is used, the fabrication success rate, R_{total} and $R_{contact}$ have been significantly improved to 90%, 26–400 kΩ μm and 10–180 kΩ μm, respectively. And through further optimization of the deposition conditions, the high success rate has been maintained and a minimum $R_{contact}$ of 1.04 kΩ μm has been measured, which are comparable to those prepared with EBM and much lower than those prepared with normal sputtering.[8,9] For comparison, Table I provides an overview of the success rate, R_{total} and $R_{contact}$ of devices prepared under different configurations

TABLE I. Summary of fabrication success rate, total resistance and contact resistance of devices prepared under different configurations and sputtering conditions.

	Normal configuration	With using shielding tube configuration	With shielding tube and optimized sputtering conditions
Successful/total devices	6/35 (17%)	18/20 (90%)	18/20 (90%)
Total device resistivity	540 kΩ μm^{-2} MΩ μm	26–400 kΩ μm	2.4–16 kΩ μm
Calculated contact resistance	260–940 kΩ μm	10–180 kΩ μm	1.04–5.4 kΩ μm

and sputtering conditions. This result appears to be contradictory to previous reports;[28,29] however, there is a reason for this as the contact metal (Au) we used was different from those in the previous reports. There are two types of contact metals, chemisorbed and physisorbed. The contact metals used in the papers were chemisorbed metals (Ti,[30] Pd, Ni, or Cu), which could react with the defective sites on graphene plane after annealing, leading to much lower contact resistance.[31] The Au contact is a physisorbed metal and has very different behavior from chemisorbed metals.[31] The reduction of contact resistance in our case is achieved via the reduction of defects in graphene underneath the metal. Based on measurements on several devices, we have also found no particular relationship between the modulation and mobility of these devices and Au deposition conditions (in the range of discharge power 20–50 W and Ar pressure 4–20 mTorr). This is because the modulation of a graphene FET depends mainly on the quality of graphene in the channel (for example, interaction between the substrate and graphene, the amount of residues on the graphene surface), and the effect of graphene quality underneath the Au contacts on the device modulation is only one of many factors.

In practice, as our DC measurement system is in an ambient environment, most of the as-prepared or cleaned devices show positively shifted Dirac points, varying from 5 to 20 V, which are in line with the effect caused by organic residuals, water and O_2 from the fabrication process, and gaseous absorption on the graphene channel.[1,32–34]

IV. CONCLUSIONS

We have demonstrated an important advance in using a shielding tube in normal sputtering configuration to address the lift-off problem during the process of practical device fabrication. With using this technique, the consequent fabrication yield rate has been significantly increased and the graphene/Au junction has been improved. The damage to graphene introduced by the sputtered Au contacts has been systematically studied, and it can be significantly reduced by either increasing the Ar pressure or decreasing the discharge power during the sputtering deposition. By taking the combined advantages of these, the interface of graphene/Au has been significantly improved, leading to the better electrical performance of graphene FET devices, such as low R_{total} and low $R_{contact}$. This work increases the choice of tools for the deposition of electrical contacts on graphene films. Further work is needed to develop a more complete understanding of the interaction of sputtered Au contacts on graphene and to optimize the contact quality while maintaining excellent electrical performance of graphene devices.

[1]K. S. Novoselov, A. K. Geim, S. V. Morozov, D. Jiang, Y. Zhang, S. V. Dubonos, I. V. Grigorieva, and A. A. Firsov, Science **306**, 666 (2004).
[2]N. Mohanty and V. Berry, Nano Lett. **8**, 4469 (2008).
[3]O. Balci and C. Kocabas, Appl. Phys. Lett. **101**, 243105 (2012).
[4]D. Wei, Y. Liu, Y. Wang, H. Zhang, L. Huang, and G. Yu, Nano Lett. **9**, 1752 (2009).
[5]J. Moser, A. Verdaguer, D. Jimenez, A. Barreiro, and A. Bachtold, Appl. Phys. Lett. **92**, 123507 (2008).
[6]X. Li *et al.*, Nano Lett. **10**, 4328 (2010).
[7]M. Okumura, S. Nakamura, S. Tsubota, T. Nakamura, M. Azuma, and M. Haruta, Catal. Lett. **51**, 53 (1998).
[8]B. Guo, Q. Liu, E. Chen, H. Zhu, L. Fang, and J. R. Gong, Nano Lett. **10**, 4975 (2010).
[9]K. Nagashio and A. Toriumi, Jpn. J. Appl. Phys. **50**, 070108 (2011).
[10]B. Dlubak *et al.*, Appl. Phys. Lett. **97**, 092502 (2010).
[11]H. M. Mohammad, K. Fang-Ling, M. Kristopher, H. Junyeon, B. Rajarshi, and D. S. Nigel, Nanotechnology **22**, 205703 (2011).
[12]F. Miriam, W. Mirosław, M. André, W. Stefan, D. Thorsten, W. Thomas, and J. A. Franz, Sci. Technol. Adv. Mater. **13**, 025007 (2012).
[13]M. Quintana, E. Vazquez, and M. Prato, Acc. Chem. Res. **46**, 138 (2013).
[14]C.-T. Chen, E. A. Casu, M. Gajek, and S. Raoux, Appl. Phys. Lett. **103**, 033109 (2013).
[15]X. P. Qiu, Y. J. Shin, J. Niu, N. Kulothungasagaran, G. Kalon, C. Qiu, T. Yu, and H. Yang, AIP Adv. **2**, 032121 (2012).
[16]Z. H. Ni, H. M. Wang, J. Kasim, H. M. Fan, T. Yu, Y. H. Wu, Y. P. Feng, and Z. X. Shen, Nano Lett. **7**, 2758 (2007).
[17]A. Reina, S. Thiele, X. Jia, S. Bhaviripudi, M. Dresselhaus, J. Schaefer, and J. Kong, Nano Res. **2**, 509 (2009).
[18]A. C. Ferrari *et al.*, Phys. Rev. Lett. **97**, 187401 (2006).
[19]L. Magdenko, F. Gaucher, A. Aassime, M. Vanwolleghem, P. Lecoeur, and B. Dagens, Microelectron. Eng. **86**, 2251 (2009).
[20]A. Venugopal, L. Colombo, and E. M. Vogel, Appl. Phys. Lett. **96**, 013512 (2010).
[21]S. Kim, J. Nah, I. Jo, D. Shahrjerdi, L. Colombo, Z. Yao, E. Tutuc, and S. K. Banerjee, Appl. Phys. Lett. **94**, 062107 (2009).
[22]W. Liu, J. Wei, X. Sun, and H. Yu, Crystals **3**, 257 (2013).
[23]K. S. Novoselov, D. Jiang, F. Schedin, T. J. Booth, V. V. Khotkevich, S. V. Morozov, and A. K. Geim, Proc. Natl. Acad. Sci. **102**, 10451 (2005).
[24]A. Reina, X. Jia, J. Ho, D. Nezich, H. Son, V. Bulovic, M. S. Dresselhaus, and J. Kong, Nano Lett. **9**, 30 (2009).
[25]P. Blake *et al.*, Solid State Commun. **149**, 1068 (2009).
[26]A. C. Ferrari and J. Robertson, Phys. Rev. B **61**, 14095 (2000).
[27]C. Vo-Van, A. Kimouche, A. Reserbat-Plantey, O. Fruchart, P. Bayle-Guillemaud, N. Bendiab, and J. Coraux, Appl. Phys. Lett. **98**, 181903 (2011).
[28]J. A. Robinson, M. LaBella, M. Zhu, M. Hollander, R. Kasarda, Z. Hughes, K. Trumbull, R. Cavalero, and D. Snyder, Appl. Phys. Lett. **98**, 053103 (2011).
[29]J. T. Smith, A. D. Franklin, D. B. Farmer, and C. D. Dimitrakopoulos, ACS Nano 7, 3661 (2013).
[30]K. Nagashio, T. Nishimura, K. Kita, and A. Toriumi, *Electron Devices Meeting (IEDM)* (IEEE, Baltimore, 2009), pp. 1–4.
[31]W. S. Leong, C. T. Nai, and J. T. Thong, Nano Lett. **14**, 3840 (2014).
[32]M. Lafkioti, B. Krauss, T. Lohmann, U. Zschieschang, H. Klauk, K. V. Klitzing, and J. H. Smet, Nano Lett. **10**, 1149 (2010).
[33]S. Mouras, A. Hamm, D. Djurado, and J.-C. Cousseins, Rev. Chim. Minér. **24**, 572 (1987).
[34]M. Ishigami, J. H. Chen, W. G. Cullen, M. S. Fuhrer, and E. D. Williams, Nano Lett. **7**, 1643 (2007).